SLAC-PEP-NOTE--176

DE88 015154

BACKGROUND SOURCES AT PEP

H. Lynch, R. F. Schwitters, W. T. Toner

ABSTRACT

Important sources of background for PEP experiments are studied. Background particles originate from high-energy electrons and positrons which have been lost from stable orbits, γ-rays emitted by the primary beams through bremsstrahlung in the residual gas, and synchrotron radiation X-rays. The effect of these processes on the beam lifetime are calculated and estimates of background rates at the interaction region are given. Recommendations for the PEP design, aimed at minimizing background are presented.

Contents

1. Introduction, Comparison of PEP with SPEAR 2
2. Beam Lifetime at PEP 3
3. Bremsstrahlung Gamma Ray Background Rate in the Interaction Region 6
4. Loss Points of Secondary Electrons from Local Bremsstrahlung . . 8
5. Secondary Electrons from Distant Bremsstrahlung 15
6. Scattered Electrons 15
7. Summary of Particle Losses Near the Interaction Point 16
8. Synchrotron X-rays 16
9. Recommendations to PEP Design Group 21
Acknowledgements 22
Appendix I: Collection of SPEAR Background Data 23

1. Introduction, Comparison of PEP with SPEAR

In looking for the main sources of background at PEP, it is natural to compare PEP with SPEAR. Some basic numbers are given in TABLE I.

TABLE I. SPEAR vs PEP

	SPEAR	PEP
Beam Energy	2.5	15
Luminosity/Burst	4.3×10^{24}	2.4×10^{26}
μ Pairs/burst	1.5×10^{-8}	2.4
Particles/bunch	10^{11}	1.5×10^{12}
Beam Lifetime	$1\text{-}2\times10^{4}$ sec	10^{4} sec
Particles lost/bunch/circuit	5	1100
Particles lost/meter/bunch	0.025	0.5
GeV lost/meter/bunch	0.0625	7.5
Synchrotron Energy loss/milliradian, bunch	4.35×10^{3} GeV	6.3×10^{6} GeV
Synchrotron Critical Energy	2.7 keV	43.8 keV

Particle losses will be substantially higher at PEP than at SPEAR and this must be taken into account in the design of the machine and the experiments. A collection of reports on background measurements at SPEAR is included in Appendix I. The main conclusions we draw are that the rates are consistent with particle loss rates due to known physical processes, but that individual measurements are very sensitive to machine tune, counter type and geometry. The most direct way to find out what will happen at PEP is therefore to compute lifetimes for PEP and estimate the distribution of particle impact points around the ring, using the PEP lattice parameters. In this report we show that it should be possible to limit the impact points of most particles lost from the ring to places well away from the 20 meter experimental regions, by installing suitably designed scrapers. Some of these methods should be able to be tested at SPEAR II.

New problems arising from the increased flux of high energy synchrotron radiation are discussed.

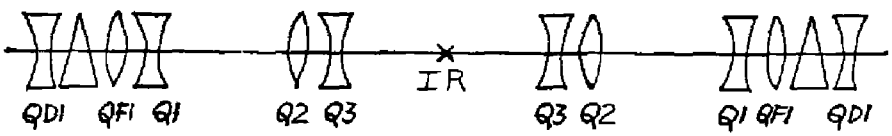

2. Beam Lifetime at PEP

(a) Beam-Gas Lifetime

Beam-gas interactions are expected to be the dominant loss mechanism for stored particles. Important processes are bremsstrahlung and coulomb scattering.

(i) Bremsstrahlung

The mechanism is: a particle suffers a bremsstrahlung collision with the gas and loses enough energy to be lost from a stable orbit. It will drift (in phase and energy) away from the RF bucket over possibly several orbital periods until it strikes the vacuum chamber. Loss rate:

$$-\frac{dn}{ndx} = \frac{\rho}{X_0} \ell n \frac{E}{\Delta E} = \frac{\ell n \frac{E}{\Delta E}}{X_0} \frac{MP}{RT}$$

$\frac{\Delta E}{E}$ = energy acceptance = 5×10^{-3}

X_0 = radiation length of gas - assumed to be CO = 38.5 gm/cm^2

M = mole weight = 28 gm/mole

P = partial pressure of CO

$$-\frac{dn}{ndx} = \frac{5.3}{38.5} \times \frac{28.\ P(10^{-9}\ \text{torr})}{171 \times 10^{14}} \times 100\ \text{m}^{-1}$$

$$= 2.25 \times 10^{-14}\ P(10^{-9}\ \text{torr})\ \text{m}^{-1}$$

beam lifetime τ is given by

$$\frac{1}{\tau} = -c \left(\frac{dn}{ndx}\right)$$

$$\tau = \frac{41\ \text{hours}}{\langle P(10^{-9}\ \text{torr})\rangle}$$

at 15 GeV, $\langle P \rangle \lesssim 10^{-8}$ torr

$\therefore\ \tau \gtrsim 4$ hours

Note that the logarithmic dependence on $\frac{\Delta E}{E}$ makes the result relatively insensitive to the size of the RF bucket.

(ii) Coulomb Scattering

The mechanism is: a particle at some position in the machine scatters in the residual gas by an angle θ; as it moves around the ring, this angle is transformed into a displacement d. When d equals a machine aperture, the particle is lost. The smallest scattering angle which can cause a particle to

strike the vacuum chamber is:

$$\theta_{min} = \frac{d}{\sqrt{\beta e\, \beta d}}$$

when d = aperture. βe = betatron function at the scattering point and βd = betatron function at d. In general, there are different values for θ_{min} in the vertical and horizontal planes. The appropriate apertures and β functions are to be used. The usual criterion for d is: $d = 10\sigma$. Thus:

$$d_V^2 = 100\,\sigma_V^2 = 100\left(\frac{\sigma_V^{*2}}{\beta_V^*}\right)\beta_V$$

$$d_H^2 = 100\,\sigma_H^2 = 100\left(\frac{\sigma_H^{*2}}{\beta_H^*}\right)\beta_V + \text{dispersion}$$

$$\frac{\sigma_V^{*2}}{\beta_V} = K^2\,\frac{\sigma_H^{*2}}{\beta_H} \qquad \beta_{ev} \approx \beta e_H \approx R/\nu$$

$$\therefore\quad \theta_V^2 = 100\,K^2\,\frac{\nu}{R}\,\frac{\sigma_H^{*2}}{\beta_H^*} \qquad \theta_H^2 = \frac{100\,\nu}{R}\,\frac{\sigma_H^{*2}}{\beta_H^*} + \text{stuff.}$$

Since $K \approx 0.28$, $\theta_V^2 << \theta_H^2$. We can neglect θ_H in what follows:

$$\theta_V^2 = \frac{8\nu}{R}\,\frac{\sigma_H^{*2}}{\beta_H^*} \qquad \frac{\sigma_H^{*2}}{\beta_H^*} = 2.5\times10^{-7}\ \text{m}$$

$$\gamma^2\theta_V^2 = 7.3 \quad @\ E = 5\ \text{GeV}$$

$$\gamma^2\theta_V^2 = 97 \quad @\ E = 15\ \text{GeV}$$

Coulomb cross section:

$$\frac{d\sigma}{d\Omega} = \frac{4r_0^2 Z^2}{\gamma^2\theta^4} \Rightarrow \sigma = \frac{4\pi\, r_0^2 Z_i^2}{\gamma^2\,\theta_V^2}$$

assuming CO is dominant residual gas,

$$\sigma \approx 86\ r_0^2 \quad @\ E = 5\ \text{GeV}$$

$$\sigma \approx 6.5\ r_0^2 \quad @\ E = 15\ \text{GeV}$$

Loss rate:

$$-\frac{1}{n}\frac{dn}{dx} = \frac{\sigma N_0 P}{RT} = \frac{86\times(2.8)^2\times 10^{-26}\times 6\times 10^{23}\times 100\times P}{1.71\times 10^{14}}$$

$$= 2.4\times 10^{-14}\times P(10^{-9}\text{ torr})\ m^{-1} \quad @\ E = 5\text{ GeV}.$$

Note @ 5 GeV the Coulomb scattering loss rate equals the Bremsstrahlung loss rate.

$$-\frac{1}{n}\frac{dn}{dx} \approx 1.8\times 10^{-15}\times P(10^{-9}\text{ torr})\ m^{-1} \quad @\ E = 15\text{ GeV}.$$

(b) Beam-Beam Bremsstrahlung

The cross section for an electron in one beam to radiate a photon in its direction of motion is:

$$d\sigma = \frac{16}{3}\alpha r_0^2\left[\ell n\left(\frac{S}{m_e^2}\right) - 1/2\right](1-y+3y^{2/4})\ \frac{dy}{y}$$

where $y = \frac{\text{Photon Energy}}{\text{Beam Energy}}$. The photons are radiated at angles of $\sim \frac{m_e}{E_0}$ to the incident electron; the degraded electrons have angles $\sim \frac{y}{1-y}\ \frac{m_e}{E_0}$ and energy $(1-y)\,E_0$. The target electron in the other beam is hardly affected at all. Both beams can radiate. At PEP

$$d\sigma = 0.665\ \ell n\left(\frac{y_{max}}{y_{min}} - 5/8\right).$$

The "γγ" group consider this as a background for tagging; with a luminosity per region per burst of 2.4×10^{26} there are 12 equivalent quanta per burst radiated in each direction and 16 $[\ell n(y_{max}/y_{min}) - 5/8]$ degraded electrons. Tagging at angles less than several times the beam divergence is clearly impossible. This process has a strong effect on beam lifetimes

$$\tau = \frac{N}{\dot{N}} = \frac{N}{L\sigma_{loss}}$$

and electrons are lost from the beam if they change energy by more than $\frac{1}{2}\%$. At PEP, with $L = 6\times 10^{32}$ for $N = 4.5\times 10^{12}$, $\tau = 2.4\times 10^4$ secs, or 6.7 hours. This is the beam lifetime, not the luminosity lifetime. In a tune shift limited machine $\Delta\nu = \text{const} \geq \frac{N}{A_{inc.}} \cdot \frac{1}{\gamma} \cdot r_0\frac{\beta_V}{2} = \frac{L}{N}\frac{1}{\gamma}r_0\frac{\beta_V}{2}$.

So that $\tau \propto \frac{1}{\gamma}$, for beam-beam bremsstrahlung.

TABLE II.

BEAM LIFETIME

LOSS MECHANISM	PARTIAL LIFETIME (hours)		ROUGH SCALING LAW
	5 GeV	15 GeV	
Beam Gas Bremsstrahlung	10 to 20	4.0	(41/P), hours
Beam Gas Coulomb Scatt.	10 to 20	51	$\propto \frac{E^2}{\langle P \rangle}$
Beam-Beam Bremsstrahlung	20	6.7	$4.5 \text{ hrs} \times \frac{N}{L}$
All causes	4 to 7	2.5	

P: Pressure of CO in units of 10^{-9} torr

E: Beam energy

N: Particles/bunch in units of 10^{12}

L: Luminosity per region in units of 10^{32}

At 15 GeV: 1200 particles per bunch, per circuit are lost:-

450 from Beam-Beam-Bremsstrahlung

750 from Beam-Gas-Bremsstrahlung

3. Bremsstrahlung Gamma Ray Background Rate in the Interaction Region

A possible source of background for experiments at PEP is bremsstrahlung where the stored beams interact with the residual gas in the long straight sections between the final bending magnets and the interaction region. The high energy gamma rays from this process will travel in a straight line from the point of production and may strike the vacuum chamber near experimental apparatus. A glancing hit will produce a shower which in turn will give numerous soft gamma rays and electrons at large angles, as illustrated in fig. 1.

We ignore the bremsstrahlung angle, and assume the angle of the gamma ray is the same as the original electron. Thus the angular distribution of the beam determines the distribution of gamma ray directions. We are interested in the rate of gammas falling on a cylindrical surface at the IR. Coordinates as defined in fig. 2.

The angular distribution of electron at Z is:

$$\frac{d^2 n_e}{dx' dy'} = \frac{N_0}{2\pi\sigma_{x'}\sigma_{y'}} \exp\left\{-\frac{1}{2}\left[\left(\frac{x'}{\sigma_{x'}}\right)^2 + \left(\frac{y'}{\sigma_{y'}}\right)\right]\right\}^2$$

The intensity of gamma rays (in units of equivalent quanta) is:

$$\frac{d^2 I}{dx' dy'} = \frac{dz}{X_0} \frac{d^2 n_e}{dx' dy'}$$

X_0 = radiation length of gas.

Now transform dx' dy' to dA at cylinder

$$\frac{\partial(x', y')}{\partial(\phi, \ell)} = \frac{r^2}{(z-\ell)^3} .$$

Equivalent gamma intensity at IR is:

$$\frac{dI}{dA} = \frac{N_0}{2\pi X_0} dZ \frac{1}{\sigma_{x'}\sigma_{y'}} \frac{r}{(z-\ell)^3} \exp\left[-\frac{1}{2}\left(\frac{r}{z-\ell}\right)^2 \left(\frac{\cos^2\phi}{\sigma_{x'}^2} + \frac{\sin^2\phi}{\sigma_{y'}^2}\right)\right].$$

Now suppose pressure and beam divergence are constant over interval between z_1, z_2, and integrate over z:

$$\frac{dI}{dA} = \frac{1}{r} \frac{N_0}{2\pi X_0} \frac{e^{-u_2} - e^{-u_1}}{\sigma_{x'}\sigma_{y'}\left(\frac{\cos^2\phi}{\sigma_{x'}^2} + \frac{\sin^2\phi}{\sigma_{y'}^2}\right)}$$

$$u_{1,2} = \frac{1}{2}\left(\frac{r}{z_{1,2} - \ell}\right)^2 \left(\frac{\cos^2\phi}{\sigma_{x'}^2} + \frac{\sin^2\phi}{\sigma_{y'}^2}\right).$$

In PEP, there are 3 such regions of interest:

(I) Q_2-Q_3: z_1 = 10 m, z_2 = 15 m; $\sigma_{x'}$ = 0.9 mr, $\sigma_{y'1}$ = 0.4 mr.
(II) Q_1-Q_2: z_1 = 15 m, z_2 = 60 m; $\sigma_{x'}$ = 0.16 mr, $\sigma_{y'}$ = 0.06 mr.
(III) QF1-Q_1: z_1 = 60 m, z_2 = 65 m; $\sigma_{x'}$ = 0.4 mr, $\sigma_{y'}$ = 0.1 mr.

Assume residual gas is CO at 5×10^{-9} torr* and there are 1.5×10^{12} particles/bunch:

*In the straight section; $\langle P_{CO}\rangle$ around the ring is $\approx 10^{-8}$ torr.

$$\left(\frac{I_0}{2\pi X_0}\right) = \frac{P(10^{-9}\ \text{torr})}{1500\,\text{m}} = \frac{1}{300\,\text{m}} .$$

The total bremsstrahlung rates in the 3 areas are:

$I_{(I)}$ = 0.15 equiv. quanta/pulse

$I_{(II)}$ = 1.5 equiv. quanta/pulse

$I_{(III)}$ = 0.15 equiv. quanta/pulse.

To estimate the rate of γ's hitting a vacuum chamber of radius 8 cm at the intersection point, we evaluate the expression for $\frac{dI}{dA}$ at $\phi = 0$, $\ell = 0$ using beam divergences twice as large as quoted in the 3 regions. The small vertical beam divergences indicate that the $\phi = 0$ rate dominates over $\phi = 90°$.

$$\frac{dI}{dA}(I) \approx 1 \times 10^{-2}$$

$$\frac{dI}{dA}(II) \approx 3 \times 10^{-5} \text{ equiv. quanta}$$

$$\frac{dI}{dA}(III) \approx 1.5 \times 10^{-2} \text{ equiv. quanta} .$$

If we average over ϕ "conservatively" ($\times \frac{1}{2}$), then the rate of γ's with energies $E > 1$ MeV, striking a beam pipe of radius 8 cm is:

0.038 per pulse per meter of length per beam.

Thus a 1 meter long cylindrical "pipe" counter placed around the interaction region could have occupancy rates as high as 7.5%. This is probably pessimistic because: (1) beam divergences were doubled, (2) energies as low as 1 MeV were counted, (3) the rate averaged over ϕ is probably less than $\frac{1}{2}$ the $\phi = 0$ rate.

For many experiments, this is not a seriously high rate. In cases where lower rates are required, better vacuum in the vicinity of QF1 and between Q2 and Q3 will help. Collimators surrounding the interaction region will be of help also.

4. Loss Points of Secondary Electrons from Local Bremsstrahlung

The electrons which radiate at the end of the curved section of the machine and in the long straight section are the most likely to cause trouble in experiments. Two cases have to be considered: (a) electrons losing only a few percent of their energy in the curved section and which can only be 'scraped'

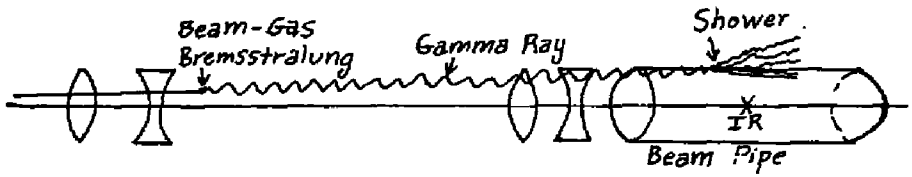
Beam-Gas
Bremsstralung
Gamma Ray
Shower
IR
Beam Pipe

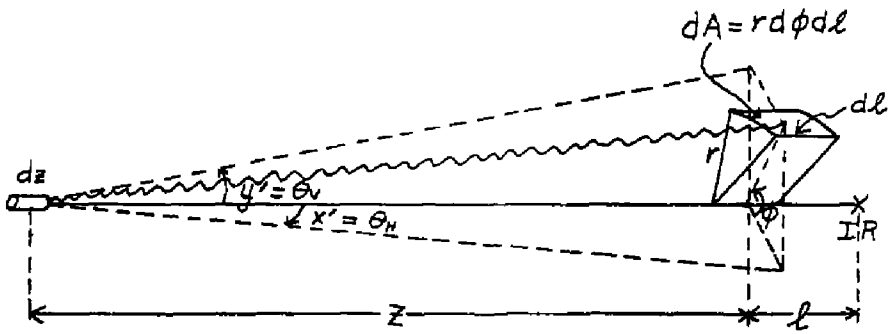
dA = rdφdℓ
dℓ
r
dz
IR
z
ℓ

Fig. 2

close to the high-β quadrupoles and (b) electrons losing a very large fraction of their energy in the straight section which are strongly deflected in the high-β quadrupoles. Some preliminary studies were made using Transport plus hand calculation. More detailed studies should be made.

(a) High energy electrons losing a small amount of energy in the region of the last bend

Ray traces of electrons which lose 1 GeV at two points in the last bend are shown in fig. 3. It can be seen that in both cases, the trajectories downstream of Q_1 are as if the electrons left the reference axis near the exit of the bend. The angular deviation in this region is proportional to the energy loss in the bend. If we define L as a distance beginning from the apparent point the track leaves the reference axis and ending where the particle hits the wall of the beam pipe somewhere near Q2, we can write:

$$\frac{h}{L} = \frac{(E_0-E)}{E} \; ; \; \frac{hdL}{L^2} = k \; \frac{E_0}{E} \; \frac{dE}{E}$$

where k is a constant depending on the bend angle and focusing properties of QF1, Q1. If the thickness of the radiator in the bend is t radiation lengths, the number of electrons of energy E is:

$$dN = tN_0 \; \frac{dE}{E_0-E}$$

and by substitution we find:

$$dN = tN_0 \; \frac{dL}{L(1+\frac{h}{kL})} = \frac{tN_0 dL}{L(1+\frac{\Delta E}{E})} \simeq tN_0 \; \frac{dL}{L} \; ,$$

since only electrons with small ΔE concern us (the others can be scraped near Q1), we can use the last expression.

For $N_0 = 1.5 \times 10^{12}$ per bunch, t ~ (length in bend)×(Pressure in 10^{-9} torr) $\times 0.44 \times 10^{-14}$, L = 50 and dL = 5, we find dN ≈ 0.16 per burst, hitting a 5 meter length of pipe just upstream of Q2, for 1.2×10^{-8} torr CO in the bend.

Note that the particles passing cleanly through Q2 are focussed in the interaction region and do not leave the beam pipe (defined to be 10 cms radius) until the quadrupoles at the exit of the interaction region are encountered.

To handle this not very frightening number of high energy electrons, a thick beam scraper (15 radiation lengths, say) should be placed upstream of Q2, arranged to shadow the pipe in Q2 from degraded particles leaving the last bend.

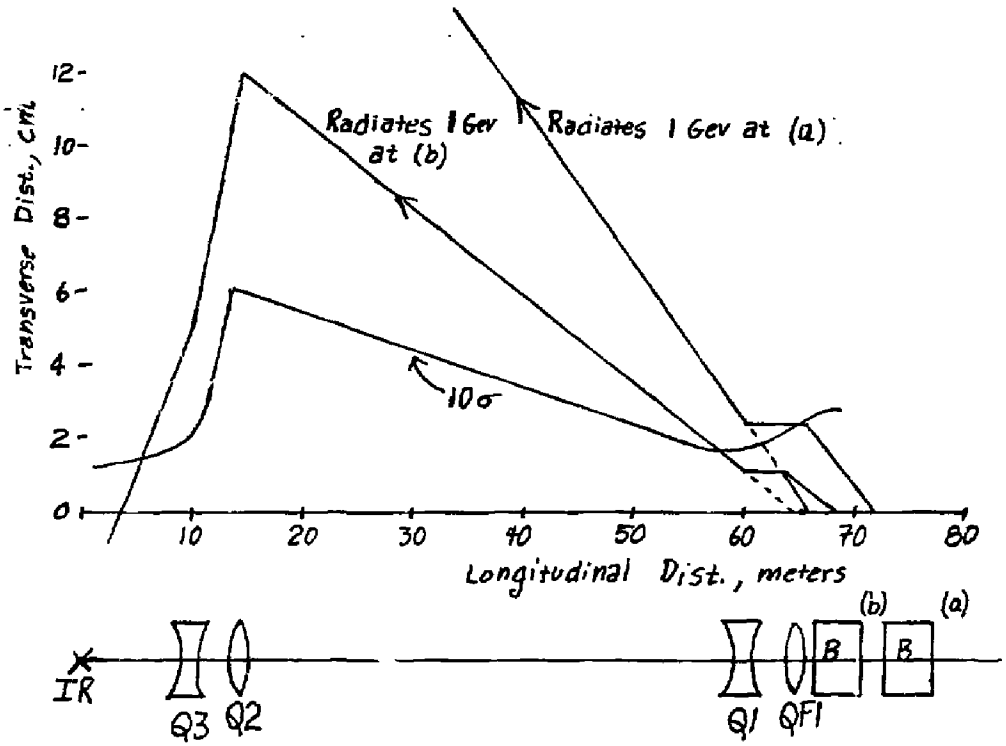
Transverse Dist., cm
12
10
8
6
4
2
0
Radiates 1 Gev at (b)
Radiates 1 Gev at (a)
10σ
10
20
30
40
50
60
70
80
Longitudinal Dist., meters
(b)
(a)
IR
Q3
Q2
Q1
QF1
B
B

Fig. 3

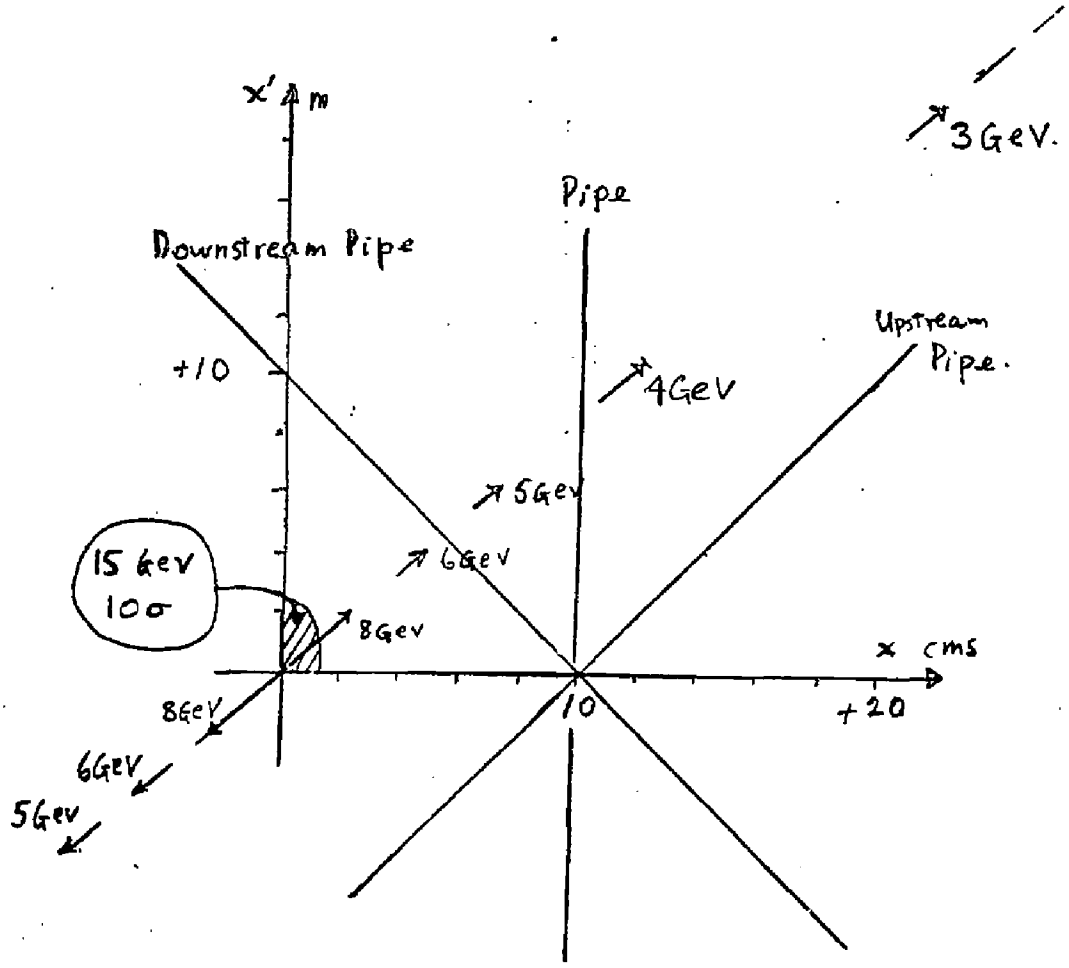

Figure 4(a) Phase space at center of interaction region (Horizontal)
Only the +ve x,x' is shown, for one beam.

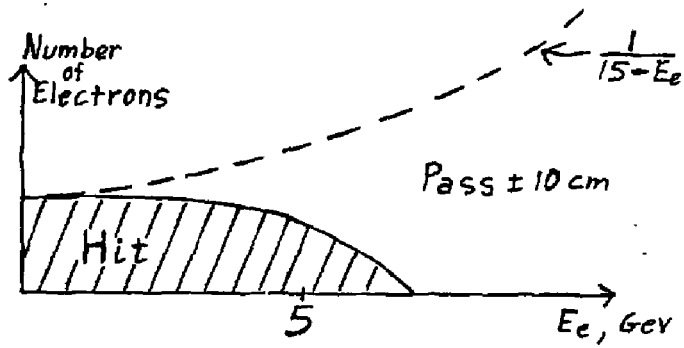
Number
of
Electrons
$\frac{1}{15-E_e}$
Pass ± 10 cm
Hit
5
E_e, Gev

Fig. (4b)

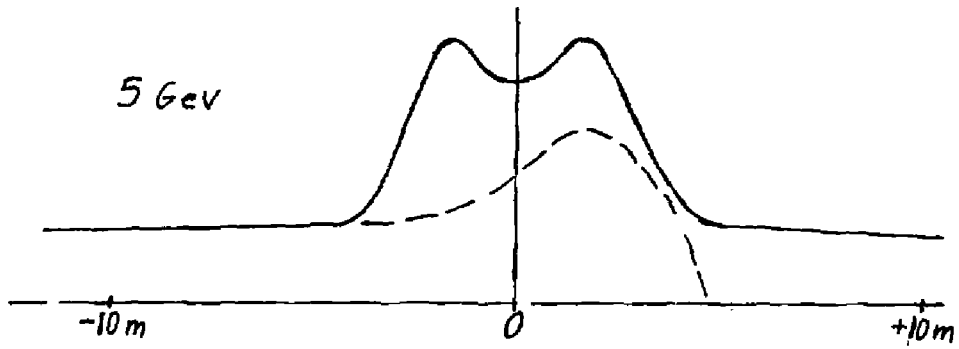
5 Gev
-10 m
0
+10 m

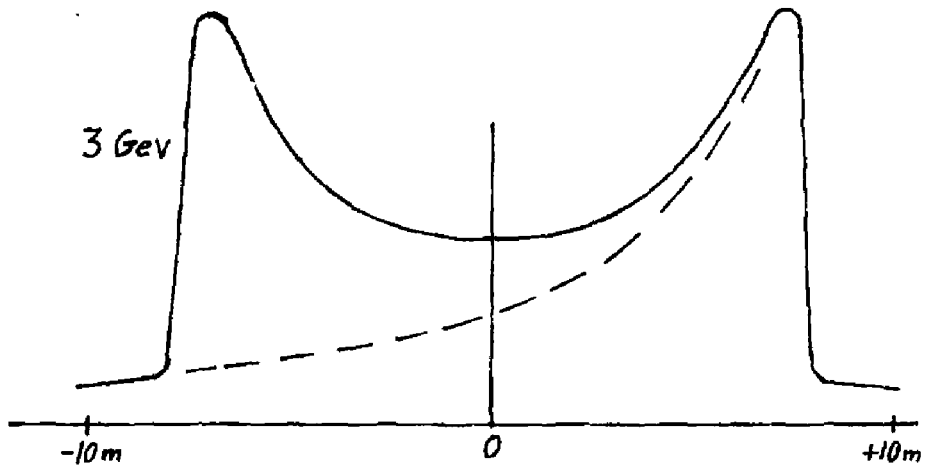
3 Gev
-10 m
0
+10 m

Fig. (4c)

If the bend upstream of QD1 is examined in a similar way, comparable numbers of particles which radiate in it can hit the pipe in the region of Q2. However, most of these can be scraped at the waist just downstream of Q1; say 50%. Thus we estimate that ~ 0.24 particles per bunch at close to full energy will have to be scraped near Q2.

(b) Electrons which lose $\geq$ 10 GeV in the straight section

Electrons which lose more than 10 GeV by bremsstrahlung in the 45 meter drift space between the matching and high-β quadrupoles do not change their trajectories significantly until they enter the high-β quadrupoles, where they are very strongly deflected in the horizontal plane. Many of them will hit the beam pipe in the 20-meter long interaction region. Vertical deflections are much less severe (because the vertical beam size in the high-β quadrupoles is less than the horizontal so that impact points on the beam pipe should be at the sides, within an inch or so of beam elevation.

Figure 4(a) shows the one standard deviation horizontal phase space at the interaction point for degraded electrons of various momenta, and the boundary set by a ± 10 cm wide, 20 meter long beam pipe.

Figure 4(b) shows the energy distribution of the particles which hit such a beam pipe. The mean electron energy is 2.6 GeV.

Figure 4(c) shows the longitudinal distribution of impact points for two momenta. The total number of electrons hitting the pipe per burst is $dN = 2 \times$ Number of Particles/bunch $\times 0.32 \times (t/X_0)$ where $(t/X_0) = P_{CO}$ (in 10^{-9} torr) $\times \ell$ (meters) $\times 0.44 \times 10^{14}$. For $P(CO) = 2.5 \times 10^{-9}$ and ℓ = 45 meters, we have 0.48 degraded electrons hitting the pipe per burst, 0.24 from each direction.

Another bad region is the 8 meter long stretch from the end of the last bend, through QF1 and Q1. Degraded electrons can be deflected in these quadrupoles, either vertically or horizontally, so that they enter the high-β quadrupoles at larger distances from the axis and are deflected through larger angles than in the case we have considered above. This raises the energy threshold for transmission through the interaction region, and also reduces the preference for loss in the horizontal plane.

A very rough estimate based on Transport runs suggests that this region generates twice as much background per unit length as the long drift space. We estimate that electrons which radiate in this region will cause 0.2 degraded electrons per burst to hit the beam pipe in the interaction region. (0.1 from each direction).

Thus the total number of degraded electrons hitting a 10 cm radius, 20 meter long, beam pipe in the interaction region is about 0.7 per burst, with energies typically 2 to 4 GeV. 70% of them will be lost at the sides of the pipe within an inch of beam elevation. The other 30% will be more or less uniformly distributed in azimuth.

The only way to improve these figures substantially is to pay for better vacuum in the long straight sections.

5. Secondary Electrons from Distant Bremsstrahlung

Beam gas bremsstrahlung in the rest of the ring and beam-beam bremsstrahlung account for the bulk of particle loss from the machine. We have seen that radiation points at the beginning of the first bend upstream of the interaction region contribute no background in the 29-meter straight section and only a small number of high energy electrons from these radiation points reach the vicinity of Q2. This will be true a fortiori of more distant points. It is only the 13% or so of particles losing between 0.5% and 1% of their energy which can come near to giving trouble. Some of these can travel many circuits of the ring before being lost. However, if a limiting horizontal aperture is placed at the horizontal waist near Q1, and a second aperture at Q2, 16 meters from the interaction point, all high energy electrons passing through them will also pass through the 20 meter interaction region without touching the walls. We estimate that at most 0.6 high energy electrons from distant bresmsstrahlung will be dumped at the aperture upstream of Q2, and believe that a careful design of beam scrapers in the curved section of the ring could reduce this substantially.

6. Scattered Electrons

In section 2(a)(ii) we saw that coulomb scattering was an important source of beam loss in 5 GeV running, the most important aperture being in the vertical plane. The scattered particles have full energy. Again, beam scrapers should be effective, this time in the vertical plane.

7. Summary of Particle Losses Near the Interaction Point

TABLE III. Summarizes the numbers given in the previous sections of the report

Radiation Point	Mean Energy	Energy Range	No/Burst (Both bunches included)	Where Dumped
		Electrons		
A	2.6 GeV	0 - 6	0.5	X
B	3 GeV	0 - 8	0.2	X
C	14.5	14 - 15	0.5	Y
Distant	14.9	> 14.7	0.5	Y
		Photons		
A & B	Bremsstrahlung Spectrum	15 GeV	0.3 equiv. quanta	X

8. Synchrotron X-rays

At PEP, the characteristic energy of a synchrotron photon is 44 keV in the standard bending magnets and 122 keV in the special polarization rotating magnets proposed by Schwitters and Richter. In addition to the well-known problem of absorbing the thermal energy, there are two new problems: the amount of lead needed to shield counters directly exposed to the synchrotron light becomes several radiation lengths, and the flux of backscattered X-rays near a dump is considerable.

We give some basic numbers here, to draw attention to the problem. Experimenters planning to use close-in tagging counters, luminosity monitors and polarization monitors will need to calculate numbers for their particular set-up.

An electron of energy E GeV loses $\frac{\Delta E}{\Delta \theta} = 4.23 \times 10^{-7} E^3 B$, GeV/radian in a field of B kilogauss. The characteristic energy of the photons is $\epsilon_c = 0.066\ E^2 B$ keV

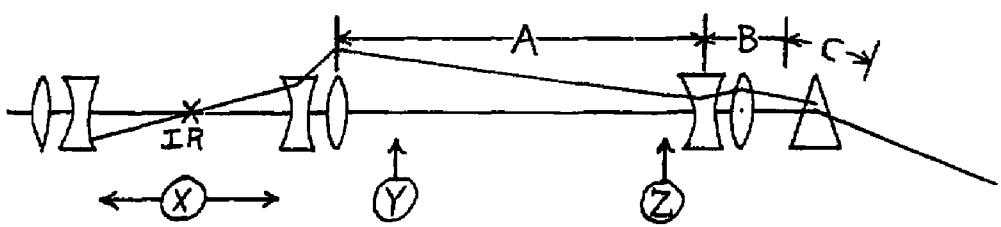

	E	B	$\frac{\Delta E}{\Delta \theta}$ per radian, electron GeV	$\frac{\Delta E}{\Delta \theta}$ per bunch, per radian GeV	ϵ_c keV
PEP	15	2.945	4.2×10^{-3}	6.3×10^{9}	43.8
		8.2	1.2×10^{-2}	1.8×10^{10}	122.0
EPIC	14	2.7	3.1×10^{-3}	2.5×10^{9}	35.4
		8.2	0.95×10^{-2}	0.76×10^{10}	107.5

The energy distribution is given in fig. 5, and attenuation curves in fig. 6, for lead.

Some examples show the magnitude of the problem.

(a) A possible geometry for a laser backscattering polarization monitor is sketched in fig. 7(a). Photons scattered at A are detected at D. Typical photon energies are 2-5 GeV. If the detector covers all vertical projected scattering angles, the resolution function of the measurement (including beam divergence) can be unfolded, and an absolute determination of the polarization made. In a typical situation, the synchrotron radiation from about 1 milliradian of the bend at B would strike the detector: 6.3×10^{6} GeV of energy, requiring 5 radiation lengths of lead to attenuate it by a factor of 10^{6}. Designs to circumvent this problem are discussed in the polarization group report.

(b) The 20 meter long wall of a 100 mm radius beam pipe in the interaction region subtends an angle of the order of half a milliradian at the bend just upstream of QF1, so 3×10^{6} GeV of X-rays will strike it from each direction, per burst, unless a collimator is placed upstream of Q2, or between Q3 and Q2. The collimator must come into $-\frac{5}{8} \times$(beam pipe radius) to shield the pipe. Apparatus in the interaction region must be shielded against X-rays scattered out of the upstream collimator, and backwards from the downstream collimator. See figure 7(b) for the geometry.

(c) Even more horrific numbers - left as an exercise to the reader - come from considering the polarization rotator proposed by Schwitters and Richter (PEP note 75). The geometry is sketched in fig. 7(c). Backscattering from the dump could be a very serious problem. It cannot be placed further downstream since the quadrupole yoke intervenes.

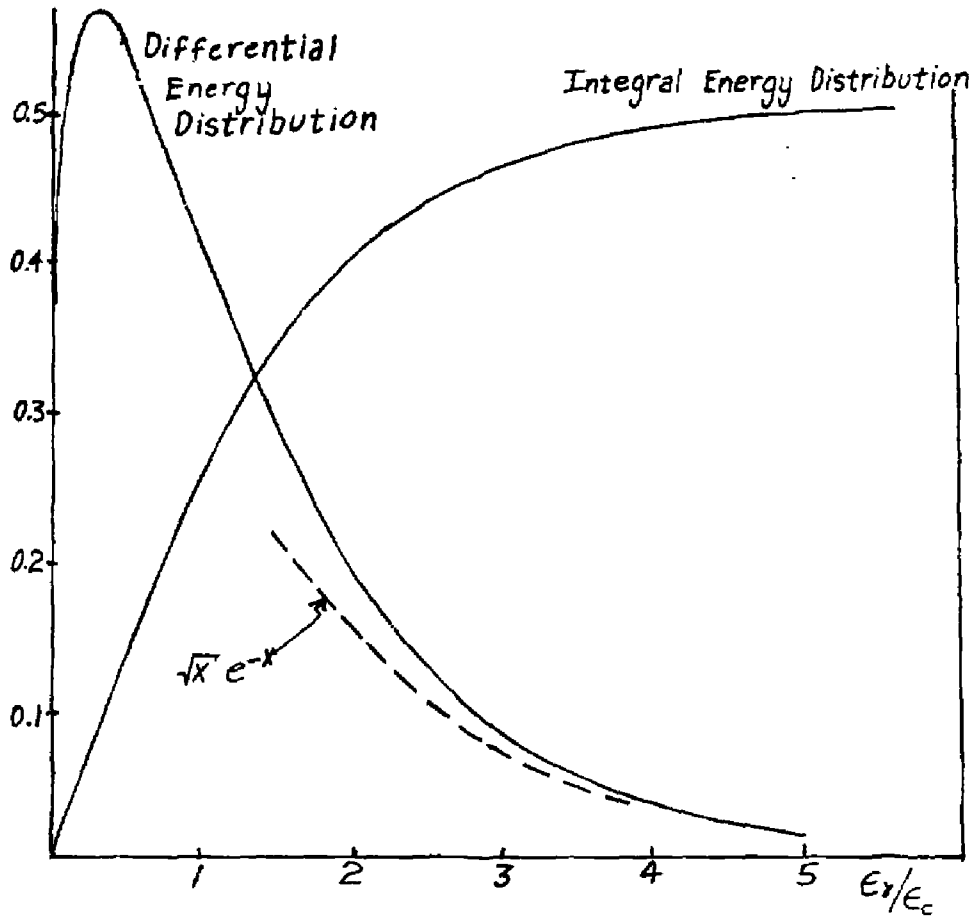
Differential
Energy
Distribution
Integral Energy Distribution
0.5
0.4
0.3
0.2
0.1
$\sqrt{x}\,e^{-x}$
1
2
3
4
5
$\epsilon_\gamma/\epsilon_c$

Fig. 5

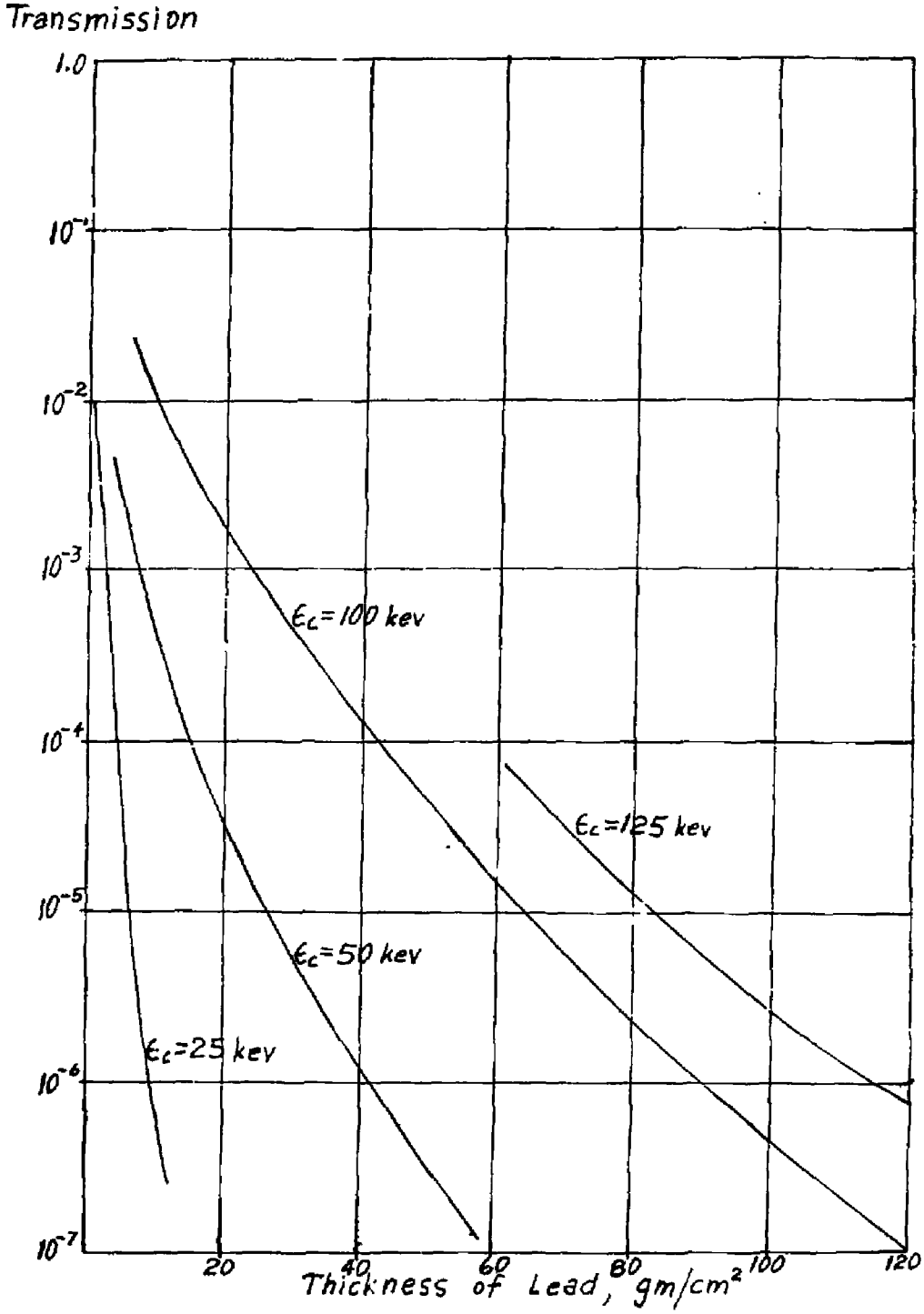
Transmission
1.0
10^{-1}
10^{-2}
10^{-3}
10^{-4}
10^{-5}
10^{-6}
10^{-7}
ϵ_c=100 kev
ϵ_c=125 kev
ϵ_c=50 kev
ϵ_c=25 kev
20
40
60
80
100
120
Thickness of Lead, gm/cm^2

Fig. 6

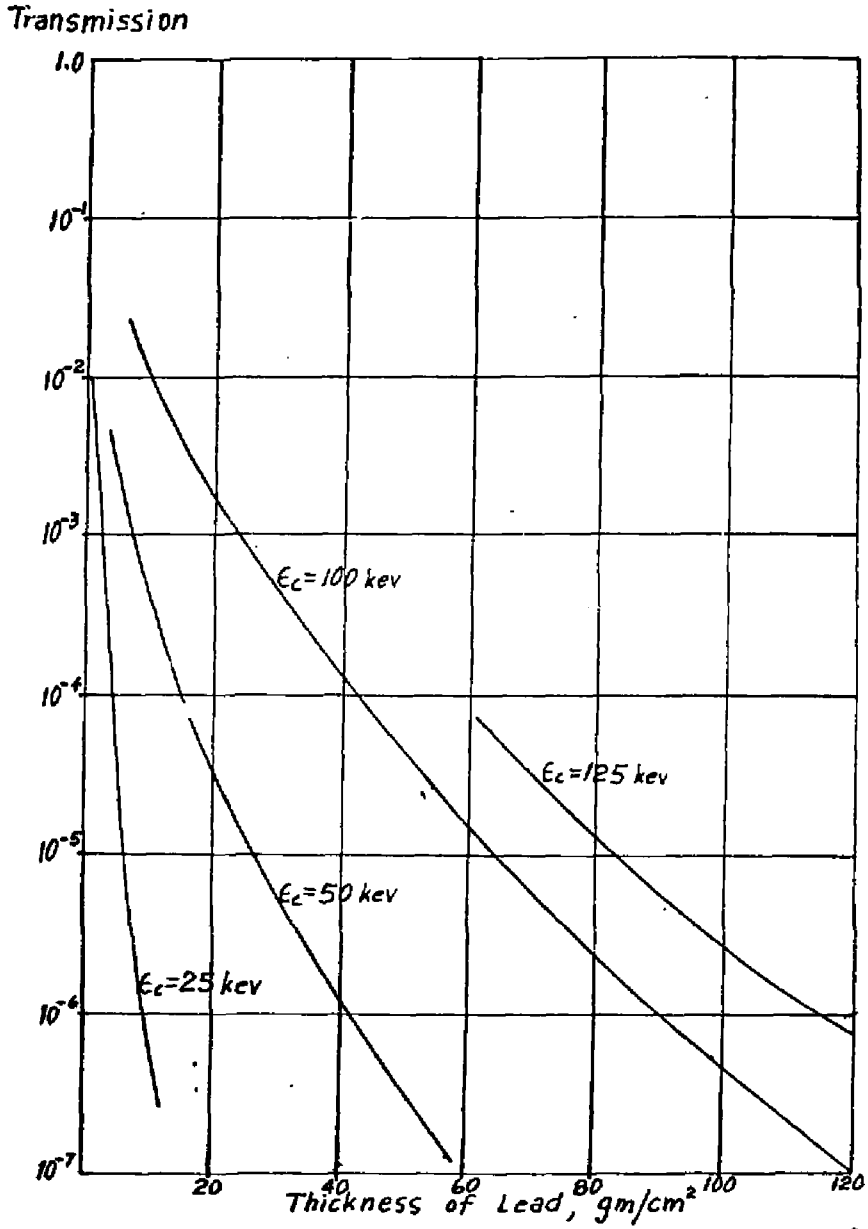
Transmission
1.0
10^{-1}
10^{-2}
10^{-3}
10^{-4}
10^{-5}
10^{-6}
10^{-7}
E_c=100 kev
E_c=125 kev
E_c=50 kev
E_c=25 kev
20
40
60
80
100
120
Thickness of Lead, gm/cm²

Fig. 6

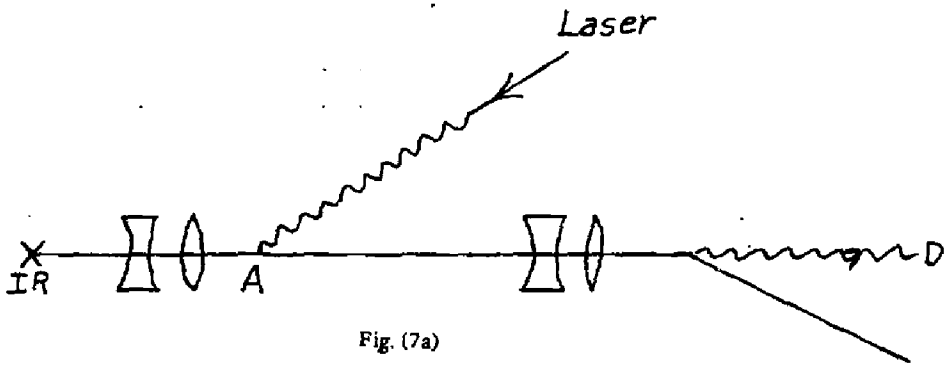

Fig. (7a)

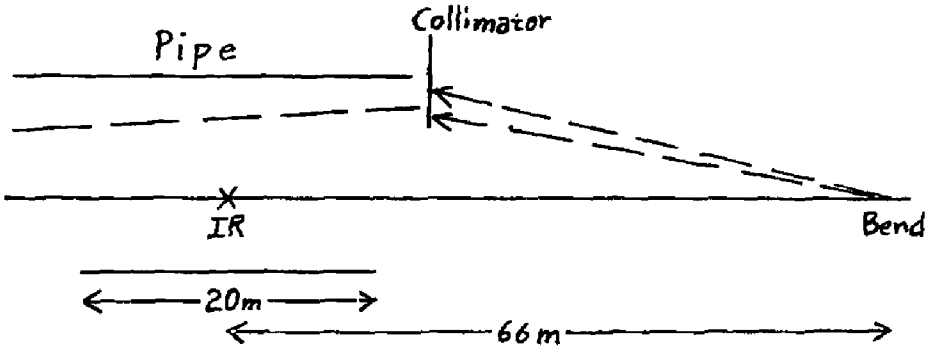

Fig. (7b)

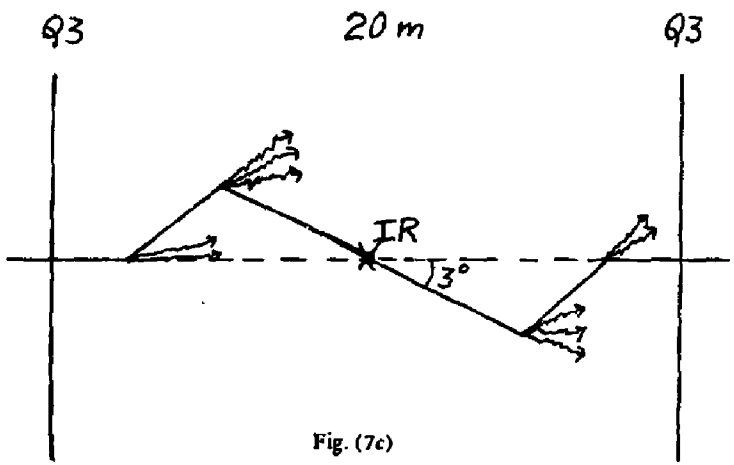

Fig. (7c)

It should be noted that the synchrotron X-ray fluxes are many orders of magnitude greater than the direct high energy particle backgrounds considered earlier in this report. Counter arrangements calculated to be especially sensitive should be tested (for example, in a SLAC beam) before installation at PEP.

We note that the production of HNO_3 in the tunnel air, and H_2 gas in the cooling water will be finite. These problems are well under control at SLAC and cause no major difficulties, but they must be remembered in the design. See the SLAC "big book". A very crude estimate suggests that free hydrogen production in the cooling water system would be ~ a few tenths of a liter per hour, easily dealt with by venting, since the water will have no induced radioactivity. Synchrotron radiation from special purpose devices like the polarization rotator is likely to be the major source of background radiation to be considered in shielding personnel.

9. Recommendations to PEP Design Group

A more extensive study of particle loss distributions in PEP should be made, and the method checked by applying it to SPEAR II. Adjustable beam scrapers will be needed at several points in the curved sections of the lattice. They need not be very thick (~ 1 radiation length) but should be near position monitors. Vertical as well as horizontal scrapers are required. Thick scrapers will be needed at 16 meters and at 55 meters from the interaction point, in the present lattice. A thick dump, designed to minimize out-scattering, will be needed to stop synchrotron X-rays from the last bend striking the vacuum pipe in the interaction region. Experimental tests of such devices in SLAC beams with 15 GeV electrons would be valuable.

It is important that the aperture of the high-β quadrupoles and the vacuum pipe through the interaction region is larger than the "shadow" of these dumps.

The residual background in the interaction region is proportional to the pressure in the straight section from the last bend to the high-β quadrupoles. Better vacuum in this region is desirable. For this reason, it seems worthwhile to concentrate the RF in one place.

The effects of any changes in the PEP lattice on backgrounds should be considered as a factor in choosing the final design.

In some experiments it will be desirable to place a lead jacket outside the vacuum pipe over most of its length in the interaction region, leaving only one or two meters at the interaction point exposed.

Some experimenters will also want to install collimators inside the vacuum chamber in the interaction region.

Acknowledgements

We would like to acknowledge useful discussions with G. Altarelli on beam-beam bremsstrahlung.

APPENDIX I

Collection of SPEAR background data

THE EFFECT OF A LOCALIZED PRESSURE INCREASE ON UNGATED SINGLES RATES IN LUMINOSITY MONITOR COUNTERS

A controlled N_2 leak was introduced in the region of G18 and 18SWI in order to study bremsstrahlung backgrounds in the West interaction region luminosity monitors of SPEAR. The leak rate was set to give a pressure "bump" in this region while the pressure and gas composition over the rest of the ring was essentially unchanged. Pressure gauges just outside the bump region (between Q2, Q3, and at 17S18) indicated that the pressure bump extended only over about 1/20 of the circumference of the ring.

A series of runs were taken at several values of the bump pressure by first adjusting the leak rate to give a stable bump pressure of the desired magnitude and then monitoring ungated singles rates as a function of beam current for single electron and positron beams under two machine configurations. The counters, "Ancient North Down" and "Ancient South Down," were used for all measurements. For every pair of singles rates measured, the beam lifetime was recorded by measuring the time required for the beam intensity to decay by 1% and the average pressure around the ring (excluding the pressure bump) was calculated by taking the average of seven vacuum gauges distributed around the ring. A machine energy of 1.5 GeV was used. The data is recorded in SPEAR Book IX, pp. 22 ff.

The expected bremsstrahlung lifetime, τ_B, is given by:

$$\frac{1}{\tau_B} = \frac{1}{I}\frac{dI}{dt} = f_o \oint ds \, \frac{\rho}{X} \ln\left(\frac{E}{\Delta E}\right)$$

where f_o is the orbit rotation frequency, ρ, X are the average density, radiation length of the residual gas, $\Delta E/E$ is the energy acceptance of SPEAR and the integral is taken around the ring. The bremsstrahlung loss rate per unit pressure over the portion of the ring excluding the pressure bump is easily calculated for the case of N_2 gas:

$$\lambda \equiv \frac{1}{\tau_B \cdot P_r} = 0.69 \times 10^{-5} \left[\beta(1-\alpha) + \alpha x\right] (\text{sec} \cdot 10^{-9}\ \text{Torr})^{-1}$$

where $x = {}^{P}/_{P_r}$, the ratio of the bump pressure to the average pressure over the rest of the ring.

α is the fraction of the circumference of the ring occupied by the pressure bump.

β is the ratio of the radiation length per unit pressure of the bump to that of the rest of the ring.

For this experiment we expect $\alpha \approx 0.06$ and $\beta \approx 1/2$ (one-half of the residual gas at base pressure is assumed to be H_2).

Coulomb scattering of beam particles on the residual gas will lead to particle loss when scattering angles are large enough to cause particles to strike the vacuum chamber. Estimates of this process* indicate that the loss rat. per unit pressure is comparable to that of bremsstrahlung. This loss mechanism gives a linear dependence on x with a slope and intercept very similar to those in the expression for λ. Particle loss coming from the Touschek effect will not be a simple linear function of x. However, extrapolating lifetime measurements to zero circulating current minimizes the Touschek contribution to λ, which, at most, should be an additive constant, independent of x.

The experimental values of λ (extrapolated to zero circulating current) versus x are shown in Figure 1. The error bars indicate the scatter in the data between runs at the same relative bump pressure, x, but under different conditions of type of beam particle and machine configuration.

As can be seen in Figure 1, the loss rate λ is consistent with being a linear function of x, but with slope and intercept some two to three times larger then those predicted by bremsstrahlung losses above. This indicates the importance of Coulomb scattering losses which may actually be the dominant loss mechanism under the conditions of this experiment.

*J.-E. Augustin private communication; 1966 SPEAR Proposal, page 106.

Figure 1

LOSS RATE PER UNIT PRESSURE

VS.

RELATIVE BUMP PRESSURE

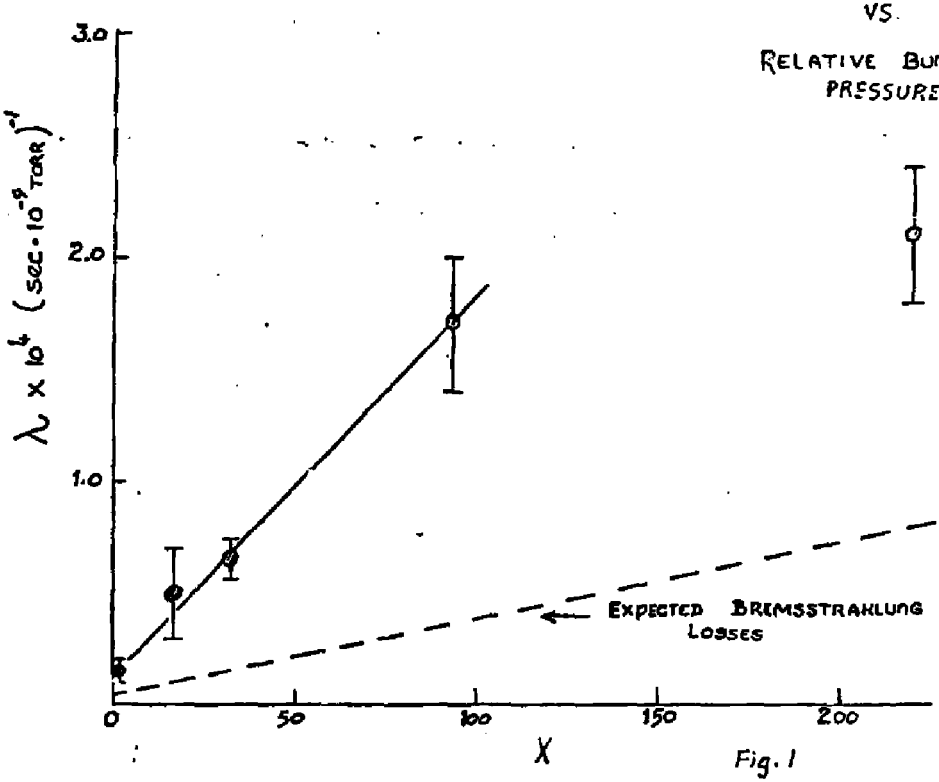

Fig. 1

Single rates data are most conveniently discussed in terms of the ϕ parameter, the number of particles counted per particle lost from the machine. This is the same parameter that was used in the Haissinski - Rees memo of 24 August, 1972. In the present case, we are interested in separating the contributions to various singles rates due to particles lost from different regions of the ring. Note that loss in this context means that the particle loses energy or is scattered in angle in the region under consideration such that some time later it will strike a physical stop in the machine and then be lost from the beam.

If the ring is divided into two regions, the pressure bump region, B, and the rest of the ring, R, then a particular ϕ_i can be written:

$$\phi_i = \frac{\text{Total counts in } i}{\text{Total Particles Lost}} = \frac{L_R \phi_{iR} + L_B \phi_{iB}}{L_R + L_B}$$

where $L_{R,B}$ are the loss rates for particles lost in the R,B regions. $\phi_{iR,B}$ (the quantities of interest) are the counts recorded in the i^{th} counter per particle lost in the R,B regions. Assuming $L_{R,B}$ are proportional to the pressure in their respective regions, then ϕ_i can be more simply written:

$$\phi_i = \frac{\phi_{iR} + (x/x_o)\,\phi_{iB}}{1 + x/x_o}$$

where x_o is a constant given by the ratio of the intercept to the slope parameter of the λ versus x function discussed previously.

The data are presented in Figures 2 and 3. Figure 2 gives ϕ's versus x for a "double-bump" configuration ($\beta_x^* = 1.20$ m, $\beta_y^* = 0.10$ m); Figure 3, a "single-bump" configuration ($\beta_x^* = 1.50$ m, $\beta_y^* = 0.10$ m). N(S) refers to th "Ancient North (South) Down" luminosity counter; +, - refer to single beams of positrons, electrons. The conditions S^+ and N^- are so-called "front-door" cases, while S^- and N^+ are "back-door" conditions. The error bars are an indication of the scatter in the data used to extrapolate the results to zero current.

At small x, the data are consistent with the results given in the Haissinski-Rees memo and demonstrate, once again, the large difference in background rates between the single- and double-bump configurations. The solid curves in Figures 2 and 3 are "eyeball" fits to the data using the formula derived above

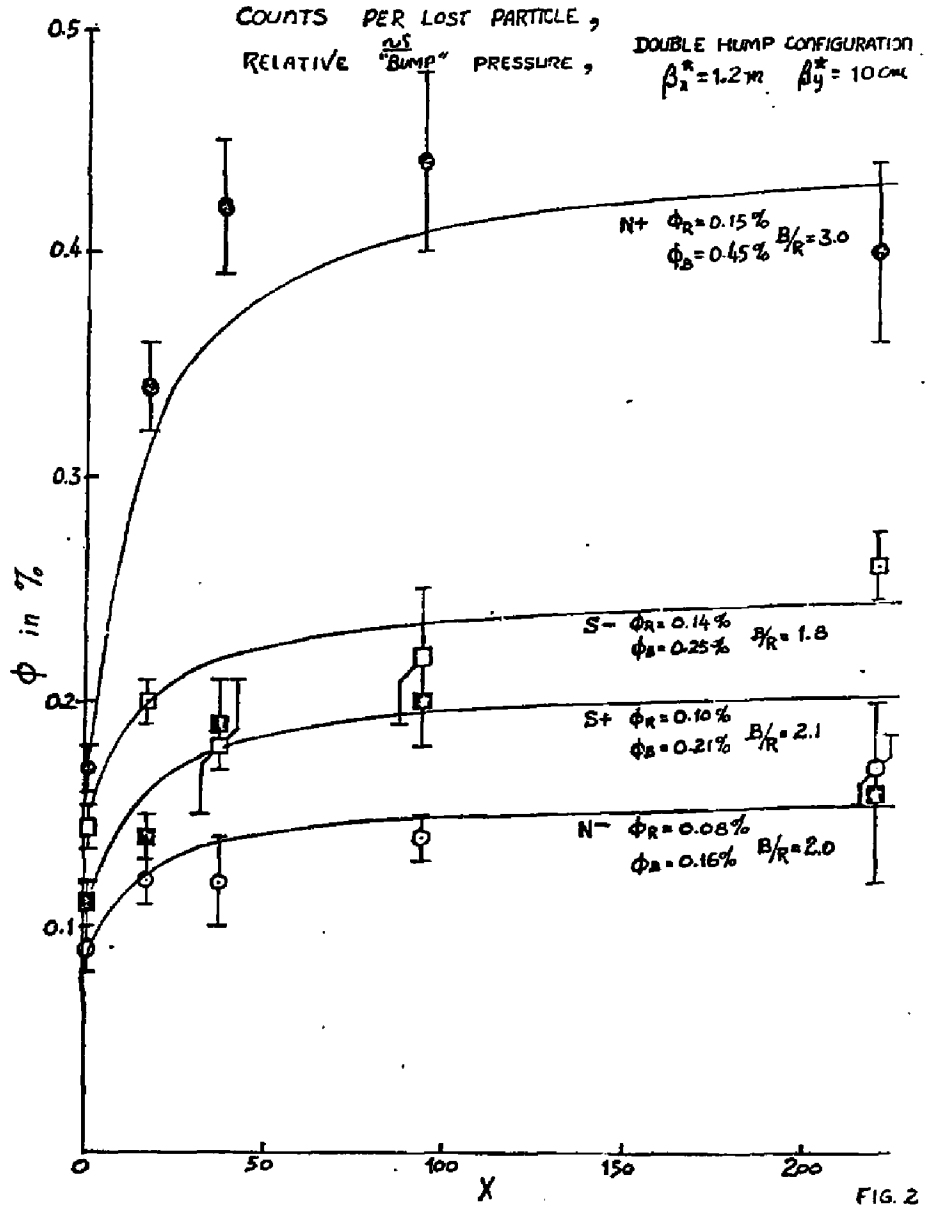
COUNTS PER LOST PARTICLE,
RELATIVE "BUMP" PRESSURE,
DOUBLE HUMP CONFIGURATION
$\beta_x^* = 1.2$ m $\beta_y^* = 100$ cm
N+ $\phi_R = 0.15\%$ $\phi_B = 0.45\%$ $B/R = 3.0$
S− $\phi_R = 0.14\%$ $\phi_B = 0.25\%$ $B/R = 1.8$
S+ $\phi_R = 0.10\%$ $\phi_B = 0.21\%$ $B/R = 2.1$
N− $\phi_R = 0.08\%$ $\phi_B = 0.16\%$ $B/R = 2.0$
ϕ in %
0.5
0.4
0.3
0.2
0.1
0
50
100
150
200
X

FIG. 2

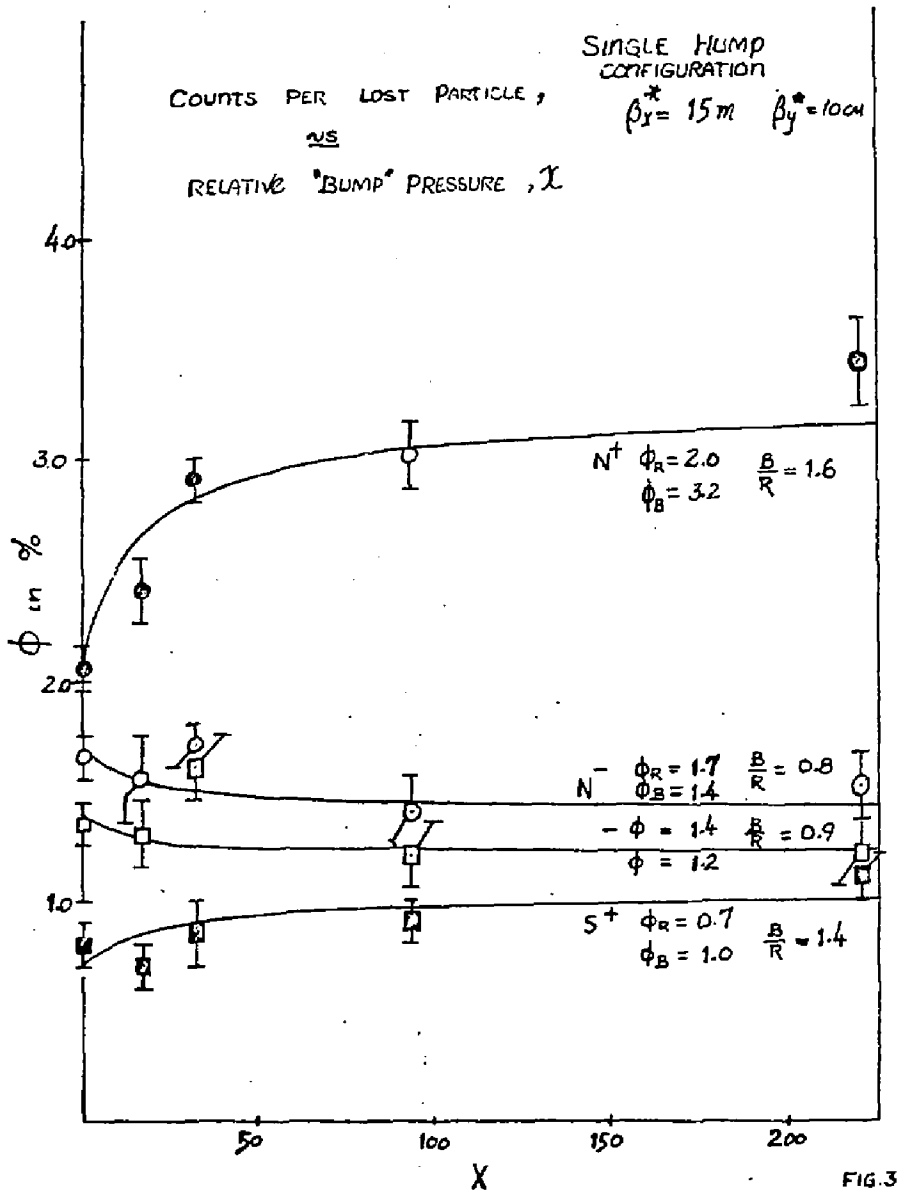
SINGLE HUMP CONFIGURATION
$\beta_x^* = 15\,m$ $\beta_y^* = 10cm$
COUNTS PER LOST PARTICLE,
VS
RELATIVE "BUMP" PRESSURE, X
ϕ in %
4.0
3.0
2.0
1.0
N^+ $\phi_R = 2.0$ $\phi_B = 3.2$ $\frac{B}{R} = 1.6$
N^- $\phi_R = 1.7$ $\phi_B = 1.4$ $\frac{B}{R} = 0.8$
$-\phi = 1.4$ $\frac{B}{R} = 0.9$
$\phi = 1.2$
S^+ $\phi_R = 0.7$ $\phi_B = 1.0$ $\frac{B}{R} = 1.4$
50
100
150
200
X

FIG.3

with $x_o = 15$. This value for x_o is in excellent agreement with that which would be obtained from the total loss rate data of Figure 1. The various values for the $\phi_{R,B's}$ are indicated on the figure. While the most striking feature of the data is the change in ϕ as a function of x for the North counter with positrons under both machine configurations, the significant result from this data is the relatively small differences between ϕ_B and ϕ_R under all conditions of type of beam and machine configuration. This means, for example, that selectively pumping the storage ring at points corresponding to where the pressure bump was in this experiment will not dramatically improve the background rates near the interaction region vacuum chambers. The special quads, Q2, Q3 with their large β values are a "catchall" for particles lost anywhere around the ring.

Supplement to
SPEAR-153
J.-E. Augustin
January 1973

The aim of this note is to show that some observations reported in SPEAR-153 can be understood if one takes into account all gas-beam interactions which are: bremsstrahlung on nuclei and electrons and elastic scattering on nuclei (elastic scattering on electrons is unimportant). The relevant cross sections can be found in J. Haissinski's Thesis (Orsay, L.A.L. 1122, Dec. 1964).

The bremsstrahlung case is properly taken care of in SPEAR-153 using the radiation lengths in gas. One may also write the cross sections:

$$\sigma_{BN} = \frac{4r_0^2 Z_i^2}{137}\,\frac{4}{3}\,\log\left(183 Z_i^{-1/3}\right)\left(\log\frac{E}{\Delta E} - \frac{5}{6}\right)$$

$$\sigma_{BE} = \frac{4r_0^2 Z_i}{137}\,\frac{4}{3}\left[\log(2.5\gamma\frac{E}{\Delta E}) - 1.\right]\left[\log\frac{E}{\Delta E} - \frac{5}{6}\right]$$

Z_i is the Z number of an atom of species i;

$\frac{\Delta E}{E}$ is the inverse of the relative rf acceptance.

For the elastic scattering on nuclei, the Rutherford cross section is $d\sigma = (4r_0^2 Z_i^2/\gamma^2\theta^4)d\Omega$, to be integrated on the ring angular acceptance. The main limit is the vertical aperture, at least if β_x is not too small. Anyway, for each motion, there is an invariant,

$$A^2 = \frac{y^2}{\beta} + \frac{(\beta\dot{y} + \alpha y)^2}{\beta}$$

At the emission one has : $x = 0$, $\dot{x} = \theta$, so that

$$A^2 = \beta_e\theta^2$$

At the loss point in the chamber wall, one has $\dot{x} = 0$, $x = a$, limiting aperture, and

$$a = \sqrt{\beta_e}\,\theta\sqrt{\beta_m}\cos\phi_j$$

It then follows that the maximum angle θ_m is given by the value:

$$\theta_m^2 = \frac{a^2}{\beta_e\beta_m}$$

Integrating the cross section over these apertures in θ_x and θ_y yields:

$$\sigma_{Ee} = \frac{4r_0^2 Z_i^2}{\gamma^2} \frac{\pi}{2} \left[\left(\frac{\beta_e \beta_m}{a^2} \right)_x + \left(\frac{\beta_e \beta_m}{a^2} \right)_y \right]$$

For SPEAR, only the y term is relevant up to now,

$$\sigma_{E\ell} = \frac{4r_0^2 Z_i^2}{\gamma^2} \frac{\pi}{2} \left[\frac{\beta_{ye} \beta_{ym}}{a_y^2} \right]$$

(the radial aperture being much bigger than the vertical one)

We can now understand :

(1) why the singles rate in luminosity countere is much worse in single-hump configuration than in double-hump configuration.

∴ the limiting aperture in single hump is the luminosity-counter notch.

One has here: a = 2.8 cm

$$\beta = .1 \left(1 + \left(\frac{2.24}{.1} \right)^2 \right) = 50 \text{ m}$$

so that $\frac{\beta_m}{a^2} = 6.4 \times 10^2 \text{ cm}^{-1}$

in Q_1, which is the only other candidate; one has

a = 2.25 cm

$$\beta = 27 \text{ m}$$

so that $\frac{\beta_m}{a^2} = 5.3 \times 10^2 \text{ cm}^{-1}$

This difference is significant, and would be balanced by any small-orbit distortion.

In the double-hump case, the limiting aperture is the Q_1 vacuum chamber:

$$\beta_{Q_1} = 72 \text{ m} \qquad \frac{\beta_m}{a^2} = 14 \times 10^2 \text{ cm}^{-1}$$

vs. the same value as before in notch: $6.4 \times 10^2 \text{ cm}^{-1}$

In this case, everything is stopped in Q_1.

(2) why the lifetime is "consistently better by ~20% in single-hump (worst background) than in double hump" (Book 9, p 34).

Let us write $\tau_j^{-1} = B + \frac{\beta_m}{a^2} E$

From the previous discussion we have:

$$\tau_{SH}^{-1} = B + \frac{6.4}{14} E = B + .45 E \quad \text{(single hump)}$$

$$\tau_{DH}^{-1} = B + E \quad \text{(double hump)}$$

From the quotation:

$$\frac{B + .45E}{B + E} = .8 \quad \Rightarrow \quad \frac{E}{B} = 0.6$$

Going back to the cross sections, one has

$$\frac{E}{B} = \frac{\pi}{2} \frac{\beta_\ell}{\gamma^2} \times 14 \times 10^2 \times 137 \times \frac{3}{4} \times \frac{1}{4.6 \times 5.2} \quad \left(\frac{E}{\Delta E} \sim 20\right)$$

$$\beta_\ell \approx \frac{R}{2} \times 7.4\,m \qquad \boxed{\frac{E}{B} \approx 0.8}$$

The agreement is better in including the electron bremsstrahlung:

if Z = 7, E/B ≈ 0.8 × (7/8) = 0.7.

The agreement is a good proof of the quality of measurements, and of the understanding of the lifetime.

As the elastic scattering goes in $1/E^2$, the lifetime should improve and the background rate difference between SH and DH should disappear in going to 2.7 GeV.

December 18, 1973

TO: SPEAR People

FROM: A. Litke and B. Sadoulet

SUBJECT: Background Rates

The enclosed table summarizes the information we have gathered on the singles rates at E=2.5 GeV. for particle detection devices placed near the beam line at SPEAR. The measurements were all done with initial luminosities $\approx 3 \times 10^{30}$ cm^{-2} sec^{-1} and initial beam currents $I_+ = I_- \approx 20$ ma. These measurements were made at different times and in different locations, so detailed quantitative comparisons would not be very meaningful. It should also be noted that the background rates at SPEAR are notoriously dependent on both the beam tune and the beam energy. The latter dependence is especially severe and not, as far as we know, understood. In particular, we do not know how to extrapolate these rates to SPEAR II energies.

With these limitations in mind, the table can serve as a rough guide. Some conclusions:

(1) Within a factor of 3, the occupancy per unit area equals 2×10^{-4} in^{-2} for all the measurements for all devices in all locations. (The occupancy is the fraction of the beam crossings for which the detector is on). This number is close to the calculated value of 1.2×10^{-4} particles lost from the beam per beam crossing per square inch of 3" radius beam pipe (assuming 40 ma. total current and a 2 hour beam lifetime).

(2) Within a factor of 2 or 3, scintillation counters, multi-wire proportional counters, and drift chambers give the same singles rates per unit area.

(3) The singles rates depend somewhat, but not dramatically, on the distance from the beam line. (Factor of 1.8 improvement in SP-4 MWPC's from 8" from the beam line out to 19"; factor of 1.4 improvement in polymeter from 4" out to 5"- but some of this may be due to more absorber between MWPC and the beam line; drift chamber sense wire rates fell a factor of 2 from 3" out to 7").

We thank B. Hughes, D. Coyne, Rudy Larsen, and G. Masek for the background rate information.

Summary of Background Singles Rates

All runs taken at E= 2.5 GeV. with luminosity $\approx 3 \times 10^{30}\,cm^{-2}sec^{-1}$
beam currents $\approx$ 20 ma. in each beam, lifetimes $\gtrsim$ 2 hrs.

Device	experiment	location	distance from beam line	dimensions	occupancy	occupancy per unit area $(inch)^{-2}$
MWPC	SP-4	vertical chamber near IR	y = 8"	Δx= 28", Δz= 28"	0.16	20×10^{-5}
			y = 10"	"	0.10	13×10^{-5}
			y = 19"	"	0.09	12×10^{-5}
MWPC (polymeter)	SP-8	2 vertical and 2 horizontal chambers around IR	x or y=3"	2 with Δx=15", Δz=72" + 2 with Δy= 6", Δz=72"	1.0	33×10^{-5}
			x or y=4"	"	0.82	27×10^{-5}
			x or y=5"	"	0.59	20×10^{-5}
counter	SP-8	vertical counter near IR	y = 6"	Δx= $1\frac{1}{2}$", Δz=28"	2.6×10^{-3}	6.1×10^{-5}
Pipe counter	SP-2	cylinder around IR	r = 5"	r= 5", Δz = 40"	0.25	20×10^{-5}
Drift chamber	La Jolla background	vertical chambers, $\perp$ to beam line, placed $\approx$ 7' upstream from IR near small angle tagging shower counters of SP-8	2"< y<8"	Δx = 1", Δy = 6"	6.2×10^{-4}	10×10^{-5}

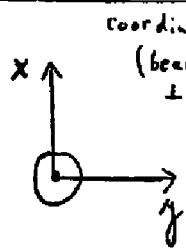

these measurements were made simultaneously

Summary of Background Singles Rates

All runs taken at E= 2.5 GeV. with luminosity≈3 x 10^{30} $cm^{-2}sec^{-1}$
beam currents ≈ 20 ma. in each beam, lifetimes ≥ 2 hrs.

Device	experiment	location	distance from beam line	dimensions	occupancy	occupancy per unit area $(inch)^{-2}$
MWPC	SP-4	vertical chamber near IR	y = 8"	Δx= 28" Δz= 28"	0.16	20 x 10^{-5}
			y = 10"	"	0.10	13 x 10^{-5}
			y = 19"	"	0.09	12 x 10^{-5}
MWPC (polymeter)	SP-8	2 vertical and 2 horizontal chambers around IR	x or y=3"	2 with Δx=15" Δz=72" + 2 with Δy= 6" Δz=72"	1.0	33 x 10^{-5}
			x or y=4"	"	0.82	27 x 10^{-5}
			x or y=5"	"	0.59	20 x 10^{-5}
counter	SP-8	vertical counter near IR	y = 6"	Δx= 1½" Δz=28"	2.6 x 10^{-3}	6.1 x 10^{-5}
Pipe counter	SP-2	cylinder around IR	r = 5"	r= 5" Δz = 40"	0.25	20 x 10^{-5}
Drift chamber	La Jolla background	vertical chambers, ⊥ to beam line, placed ≈ 7' upstream from IR near small angle tagging shower counters of SP-8	2"< y<8"	Δx = 1" Δy = 6"	6.2 x 10^{-4}	10 x 10^{-5}

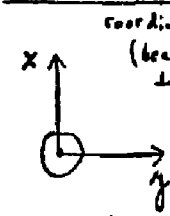

these measurements were made simultaneously